Cloning and functional analysis of the promoter of SinSyn gene in Sinomenium acutum

Meilin An

1445019640@qq.com

Hunan Agricultural University

Bing Li

Hunan Agricultural University

Jiabei Chen

Hunan Agricultural University

Xiyao Zeng

Hunan Zhengqing Pharmaceutical Group Co., Ltd

Xinbo Chen

Hunan Agricultural University

Hua Yang

Hunan Agricultural University https://orcid.org/0000-0003-3651-7282

Research Article

Keywords: sinoacutine synthetase, Sinomenium acutum, promoter, hormone, abiotic stress

Posted Date: July 3rd, 2024

DOI: https://doi.org/10.21203/rs.3.rs-4564332/v1

Abstract

Sinoacutine synthetase (SinSyn) is one of the key enzymes in the biosynthesis pathway of sinomenine (SIN), an effective pharmacological component in *Sinomenium acutum*. However, the transcriptional regulation mechanism of this gene in the SIN synthesis pathway has not been studied. In this study, a 1520 bp upstream promoter sequence and three 5' terminal truncations were used to drive the *GUS* reporter gene to test their activities in transiently expressed tobacco and stable transgenic *Arabidopsis*. Both the full-length promoter and the truncated promoters can initiate GUS expression. As the 5' end is removed, their activity is different. The results of GUS histochemical staining showed that − 956 bp ~ -622 bp was an important position of *SinSyn* gene promoter. In addition, bioinformatics analysis revealed that various regions of the *SinSyn* promoter were distributed with some abiotic stress and plant hormone activation. Through transgenic *Arabidopsis thaliana* verification, it was confirmed that the *SinSyn* gene promoter could respond to methyl jasmonate (MeJA), auxin (NAA, IBA), drought, and NaCl. The MeJA response elements were located at -1520 bp ~ -956 bp, the auxin response elements were located at -622 bp ~ -395 bp, the drought response elements were located at -395 bp ~ -1 bp and the NaCl response elements were located at -956 bp ~ -1 bp. In general, our study provides a theoretical reference for the application of *pSinSyn* in biological stress resistance, the functional verification of the *SinSyn* gene, and the regulation of SIN synthesis in *Sinomenium acutum*.

Key Message

The promoter of the *SinSyn* gene was successfully cloned, and some of its functional elements were verified. This study aims to provide a theoretical reference for investigating the molecular function and mechanism of the *SinSyn* gene.

Introduction

The promoter is the 5' upstream DNA sequence of a structural gene and is an important part of the gene (Zhu, et al. 2010). Plant promoters are located upstream of the initiation codon ATG, which can activate RNA polymerase II and bind specifically to transcription factors, thereby determining a crucial control point in gene transcription. At the same time, promoters also regulate the timing and level of gene expression in organisms (Kummari, et al. 2020). Therefore, isolation and identification of promoters are particularly important for exploring the molecular mechanisms of gene expression. At present, an increasing number of gene promoters have been isolated and identified from many plants. Chen and Qiu cloned the promoter of the nucleotide exchange factor *ZjFes1* and studied its expression in tissues under high-temperature stress. It was found that the expression of *ZjFes1* increased significantly at 1 h after high temperature, suggesting that the gene promoter may contain a high temperature response element that has not been identified (Chen and Qiu. 2020). Li et al. cloned the promoter sequence of 2398 bp upstream of the *LkF3H2* gene, and determined that the key promoter region was located between − 526 bp and − 429 bp, and the promoter could respond to MeJA, ABA, NaCl, and low temperature (Li, et al. 2023). Wang et al. cloned the promoter sequence of the *DcCDPK8* gene in

Dendrobium, and found that the gene promoter was involved in the signal transduction of low temperature stress, hormone ABA and MeJA (Wang, et al. 2019).

Sinomenium acutum is a traditional Chinese medicine mainly used for treating rheumatoid arthritis (Zhang, et al. 2022) (Gong, et al. 2023). *Sinomenium acutum* exhibits pharmacological effects due to its high alkaloid content, with the most prevalent one being sinomenine (SIN). SIN is one of the isoquinoline alkaloids known for its various pharmacological activities, including anti-inflammatory (Gao, et al. 2021), analgesic (He, et al. 2017), anti-cancer (Li, et al. 2023), immunosuppressive (Wang, et al. 2023) and treating rheumatoid arthritis (Liu, et al. 2018). At present, research on SIN mainly focuses on its pharmacological effects, with few studies on its biosynthesis. In our previous *Sinomenium acutum* transcriptome data analysis, the upstream pathway of SIN synthesis was proposed (Zeng, et al. 2019). The *SinSyn* gene was cloned based on the transcriptome data and whole-genome data of *Sinomenium acutum*. The heterologous expression SinSyn protein in *Saccharomyces cerevisiae* was determined that can catalyze S-reticuline to sinoacutine (Chen, et al. 2024) (Fig. 1). Sinoacutine plays an important role in the synthesis of SIN. However, the regulatory mechanism of the *SinSyn* gene, which catalyzes the formation of sinoacutine from S-reticuline, is still unclear.

In this study, a 1520 bp *SinSyn* gene promoter was isolated and analyzed from the genomic DNA of *Sinomenium acutum* using nested PCR. In order to identify the function of the *SinSyn* promoter, the full-length promoter and three 5' terminal truncated fragments were used to drive *GUS* gene expression in tobacco and transgenic *Arabidopsis thaliana*. Firstly, GUS staining was used to determine whether the promoter had tissue-specific expression, and then real-time fluorescence quantitative PCR (qRT-PCR) was used to analyze its plant hormone and abiotic stress-induced active regions. These results provide a deeper insight into the transcriptional regulation of the *SinSyn* gene and serve as a theoretical reference for studying the molecular function and mechanism of the *SinSyn* gene.

Materials and Methods

Plant Materials and growth conditions

In this study, the two-year-old *Sinomenium acutum* cultivated at the cultivation base of Zhengqing Group in Huaihua City, Hunan Province, was used as the material. Wild-type *Nicotiana tabacum* seeds were cultured under 16/8 h light/dark, 6500 lx, 28 ± 2°C. The *Arabidopsis* Col-0 seeds were disinfected with 75% ethanol for 15 min and then cleaned. Subsequently, sterile seeds were sown on Murashige-Skoog (MS) solid medium, and then aseptically cultured for one week under a 16/8 h light/dark, 2000 lx, at 22 ± 2°C. The seedlings were then transferred to a seedling substrate for 2 weeks.

Strain and vector

Plant expression vector pCAMBIA1301 was purchased from Beijing Huayueyang Biotechnology Co., Ltd. *Escherichia coli* (*E. coli*) competent DH5α was purchased from Beijing Jingke Biotechnology Co., Ltd., *Agrobacterium tumefaciens* GV3101 was purchased from Shanghai Weidi Biotechnology Co., Ltd..

Promoter cloning and sequence analysis

Genomic DNA was extracted from young leaves of *Sinomenium acutum* using the Hi-DNAsecure Plant Kit (Tiangen, Beijing, China). The DNA quality was assessed using a micro-spectrophotometer, and the integrity was evaluated through 1% agarose gel electrophoresis. From the whole genome data of *Sinomenium acutum* (not yet published), the software TBtools extracted the upstream 1700 bp and downstream 150 bp of the *SinSyn* gene. According to the principle of nested PCR, forward primers with a *Bam*HI restriction site and aattcgagctcggtacccgg homologous arm, and reverse primers with an *Nco*I restriction site and ttaccctcagatcta homologous arm were designed for promoter amplification. The primers are shown in Table 1. The first round of nested PCR conditions was as follows: pre-deformation (98°C) 2 min, denaturation (98°C) 10 s, annealing (53°C ~ 56°C) 15 s, extension (72°C) 30 s, 35 cycles of denaturation, annealing and extension, final extension (72°C) 5 min, preservation (4°C) ∞. The product of the first round of PCR was used as a template for the second round of PCR, and the reaction conditions remained the same as described previously. The amplified products were detected by 1% agarose gel electrophoresis, purified by *EasyPure*® Quick Gel Extraction Kit (TransGen Biotech, Beijing, China), and stored at -20°C. The amplified promoters were named *SinSyn*-1520-p0, *SinSyn*-956-p1, *SinSyn*-622-p2, and *SinSyn*-395-p3, referred to as p0, p1, p2, and p3.

The transcription start site and a core fragment of *pSinSyn* were predicted by Berkeley Drosophila Genome Project (BDGP). The cis-acting components of *pSinSyn* were predicted by PlantCARE (http://bioinformatics.Psb.ugent.be/webtools/plantcare/html/) (Rombauts, et al. 1999).

Vector construction

The recombinant vector was constructed using a homologous recombination kit (TransGen Biotech, Beijing, China). The four promoter fragments obtained by amplification were inserted into the plant expression vector pCAMBIA1301, which had been digested by the restriction enzymes *Bam*HI and *Nco*I (Fig. 2). The amount of each component in the reaction system was calculated according to the kit instructions, and a series of recombinant vectors were constructed. The reaction was carried out at 50°C for 15 min in a PCR instrument. After the reaction, it was immediately placed on ice to cool for several seconds. The obtained homologous recombination products were named pCAMBIA1301-p0::*GUS*, pCAMBIA1301-p1::*GUS*, pCAMBIA1301-p2::*GUS*, pCAMBIA1301-p3::*GUS*, referred to as Q0, Q1, Q2, Q3. The recombinants were transformed into DH5α competent cells by freeze-thaw method for amplification. The plasmid pCAMBIA1301, containing the CaMV35S promoter-*GUS*, was used as the positive control vector. The extracted positive single colony plasmid was sent to Beijing Qingke Biotechnology Co., Ltd. for sequencing. After comparing the sequencing results, the correct recombinant plasmid was transformed into *Agrobacterium tumefaciens* GV3101 competent cells using the freeze-thaw method. After coating on YEB Kan and Rif solid medium, single colonies were picked and verified by colony PCR. The correct positive single colonies were stored at 4°C.

Table 1 Primers used in this study

Primer name	Sequence of primer（5' - 3'）	Function
pSinSyn-F	TTGGGCATTTCGCATCACCTC	Nested PCR first round amplification with promoter primers
SinSyn-R	GTGGCATGGGTGCATATCTAG	
SinSyn-1520-F(p0-F)	aattcgagctcggtacccggggatccTCTGACAAACAAGGACCGTTGAT	Nested PCR second round amplification with promoter primers
SinSyn-956-F(p1-F)	aattcgagctcggtacccggggatccGTAAGCACCATTACGGGACAAAT	
SinSyn-622-F(p2-F)	aattcgagctcggtacccggggatccGCATACACAGAGTTCATCAGGAAT	
SinSyn-395-F(p3-F)	aattcgagctcggtacccggggatccGACCAAGGAAAAGGTACTGCTAAT	
SinSyn-1520-R (p-R)	ttaccctcagatctaccatggTTCAGAGGTTTTGATTGCGTTCT	
M13-F	CAGGAAACAGCTATGACC	Universal primers for vector
M13-R	TGTAAAACGACGGCCAGT	
pCAMBIA1301-F	ATTAGGCACCCCAGGCTTTACAC	Colony PCR primers and transgenic positive seedling validation primers
pCAMBIA1301-R	ACGGGTTGGGGTTTCTACAGGAC	
U6- qRT-F	CGATAAAATTGGAACGATACAGA	Internal reference gene
U6- qRT-R	ATTTGGACCATTTCTCGATTTGT	
GUS-qRT-F	CGACTGGGCAGATGAACAT	Fluorescence quantification
GUS- qRT-R	ATACTCCACATCACCACGCT	

Note: "_____ " is the added enzymatic site sequence; "~~~~~ " is the added homology arm sequence.

Transient transformation of tobacco

Agrobacterium positive clone was inoculated in 4 mL Yeast Extract Peptone Broth Medium (YEB) liquid medium containing 50 μg/mL kanamycin and 25 μg/mL rifampicin, and cultured at 28°C 200 r/min for 48 h. 1 mL of bacterial solution was centrifuged at 5000 r/min for 5 min to collect bacteria. Wash the bacteria with fresh resuspension (10 mM $MgCl_2$, 2% sucrose, and 10 mM MES, pH 5.6) (Dong, et al. 2023) (Monika, et al. 2016), repeat 3 times. Finally, the bacteria were resuspended, 0.2 mM AS was added to the resuspension, and the OD600 was adjusted to 0.2–0.35. The bacterial solution was incubated at room temperature for 2–3 h, and protected from light. Subsequently, the lower epidermis of tobacco leaves was injected and marked. The labeled leaves were immediately transferred into dark culture for 24 h. After normal photoperiod culture for 24–48 h, samples were collected for GUS tissue staining, *GUS* gene expression analysis, and enzyme activity determination.

GUS tissue staining analysis

The GUS tissue staining kit (Coolaber, Beijing, China), was used for the staining analysis. The samples were immediately immersed in the staining solution and subjected to vacuum pumping for 30 minutes. Subsequently, they were incubated in the dark at a temperature range of 30–37°C. The staining time varied from 12 to 36 h depending on the tissues and organs. Subsequently, 75% ethanol was utilized for decolorization and preservation to facilitate further observation and photography.

GUS activity analysis

Samples for GUS activity were ground into a powder with liquid nitrogen, and about 100 mg was transferred to the EP tube, and 1 mL of GUS enzyme extract (Blázquez 2007) was promptly added. The mixture was vortexed, centrifuged at 12,000 rpm at 4°C for 5 min, and the supernatant was then transferred to a new EP tube for use in an ice bath. The protein concentration of each sample was determined by Bradford method to measure the absorbance at 595 nm, and was calculated by BSA standard curve (Kielkopf, et al. 2020). Finally, the GUS protein activity was quantitatively detected according to Jefferson et al. (Jefferson, et al. 1987). 100 μL of protein supernatant was taken to a light-proof microplate, and 400 μL of GUS extraction buffer preheated to 37°C was added. Then, 500 μL of 2 mmol/L MUG substrate reaction solution was added and mixed, and incubated at 37°C. 100 μL of mixed reactants was mixed with 400 μL of 0.2 mol/L Na_2CO_3 termination solution at 0 min and 60 min, respectively. The fluorescence intensity was measured at an excitation wavelength of 365 nm and an emission wavelength of 455 nm. The concentration of 4-MU produced by each sample reaction was obtained through the 4-MU standard curve, and the GUS activity (4-MU nmol/min/mg) was calculated. Three repeated experiments were designed for each sample. The error bar represents the mean ± standard error.

Stable transformation of Arabidopsis thaliana

The genetic transformation of *Arabidopsis thaliana* was carried out using the *Agrobacterium* inflorescence infection method (Clough and Bent 1998) (Ali, et al. 2022). Transgenic *Arabidopsis* plants were generated by the floral dip method. The fresh GV3101 *Agrobacterium* solution of Q0, Q1, Q2, and Q3 expression vectors was prepared. The bacteria were suspended in the fresh infection solution (100 mL infection solution: 0.211 g MS medium, 5 g sucrose, 0.05 g MES, pH adjusted to 5.7–5.8 with KOH, 1 μL of 6-BA at a concentration of 1 mg/mL, and 15 uL SilwetL-77). The *Arabidopsis* inflorescence was immersed in the infection solution for 1 min and then properly dried. After infection, it was cultured in the dark for 24 h, followed by normal photoperiod culture. Generally, the infection was carried out 2–3 times during the full-bloom stage, with an interval of 1 w each time, and the seeds were cultured normally until harvest in the later stage. Positive transgenic seedlings were screened by germinating the transgenic seeds on MS solid medium containing 25 mg/L Hyg. The Hyg resistance seedlings were transferred to the soil. After 2 weeks, the appropriate number of leaves were taken, and the DNA of *Arabidopsis* leaves was extracted by CTAB method (Monika, Parul, Sanjay and Singh 2016) (Mavrodiev, et al. 2021). The transgenic A*rabidopsis thaliana* was further confirmed by PCR. The amplification procedure was as

follows: pre-deformation (95°C) 2 min, denaturation (95°C) 10 s, annealing (54°C) 15 s, extension (72°C) 30 s, denaturation, annealing and extension 30 cycles, final extension (72°C) 5 min, preservation (4°C) ∞. The products were amplified by Bio-Red PCR instrument and primers pCAMBIA1301-F and pCAMBIA1301-R (Table 1).

Hormone and abiotic stress treatments of transgenic Arabidopsis thaliana

Based on the predicted functions of some of the action elements in the promoter of the *SinSyn* gene and the range of the intervals in which they are located, Q0 transgenic *Arabidopsis thaliana* (predicted to contain MeJA response elements) was sprayed with 100 μM MeJA. And Q2 transgenic *Arabidopsis thaliana* (predicted to contain NAA and IBA response elements) was sprayed with 100 μM IBA and NAA. Q1 (without MeJA response elements) and Q3 transgenic *Arabidopsis* (without auxin response elements) and wild-type *Arabidopsis* were used as controls for the same treatment. The treated transgenic *Arabidopsis* materials were sampled at 6 time points of 0, 4, 8, 12, 24, and 48 h, and then frozen in liquid nitrogen. The samples were ground into powder by automatic plant tissue crushing instrument, and then the total RNA of plant samples was extracted for the detection of *GUS* gene expression.

RNA extraction and real-time fluorescence quantitative analysis (qRT-PCR)

Total RNA was extracted by FreeZol Reagent (Vazyme, Nanjing, China), genomic DNA was removed, and cDNA was synthesized with HiScript□Q RT SuperMix for qPCR (+ gDNA wiper). The 10-fold diluted cDNA was used as a template, U6 was employed as an internal reference gene, and *GUS* was utilized as a detection gene for qRT-PCR. Each sample contains 3 biological replicates and 3 technical replicates. System for qRT-PCR in 10 μL: 2 × ChamQ SYBR qPCR Master Mix 5 μL, upstream and downstream primers 0.2 μL, cDNA 0.5 μL, ddH_2O 4.1 μL. PCR reaction conditions: predenaturation at 95°C for 3 min, denaturation at 95°C for 10 s, 40 cycles, annealing & extension at 55°C for 30 s, and a dissolution curve from 65–95°C at a rate of 0.5°C / 5 s. The relative expression of genes was calculated using the 2^(-ΔΔCt) method.

Statistical analysis

In order to verify whether there was a significant difference between the mean values, a two-way ANOVA analysis was conducted using the software GraphPad Prism 8. The data were analyzed using Tukey's multiple comparison test, which revealed three independent replicates of mean ± SE. * and ** represent significant differences at the 0.05 and 0.01 levels.

Results

Cloning and bioinformatics analysis of SinSyn promoter

A 1520 bp promoter sequence (Fig. 3a) and three 5' truncated fragments (Fig. 3b) upstream of the *SinSyn* gene ATG were cloned through nested PCR after two rounds of PCR reactions using the genomic DNA as a template. They are referred to as p0, p1, p2, and p3, respectively. As predicted by BDGP, the upstream sequence of the *SinSyn* gene had six possible core promoter regions, which were located at -77 bp ~ -27 bp, -318 bp ~ -268 bp, -412 bp ~ -362 bp, -783 bp ~ -733 bp, -1258 bp ~ -1208 bp, -1173 bp ~ -1123 bp (Table 2). Based on the prediction results of PlantCARE (Fig. 3c), the core promoter elements of the promoter sequence include 14 TATA-boxes (Table 3), which can drive the transcription initiation complex to start transcription at the correct position, and 22 CAAT boxes (Table 3), which are common cis-acting elements in the promoter enhancer region and are related to the transcription initiation frequency (Shirsat, et al. 1989). In addition, it also contains a variety of cis-acting elements, including light-responsive elements (TCT-motif, Box 4, AAAC-motif, GATA-motif), hormone-responsive elements (CGTCA-motif, AuxRE), stress-responsive elements (MYB recognition site, CCAAT-box, TC-rich repeats, MYC). The prediction results showed that the promoter was regulated by a variety of external factors, which provides a theoretical basis for further study on the regulation mechanism of the *SinSyn* gene.

Table 2
Predicted transcription initiation site in the *SinSyn* promoter

Start	End	Score	Promoter Sequence
-77	-27	0.88	CTAACTCACTCCTATAAATGCCATCTCCCATCTTTCCCTA**A**CTTCTTCAA
-318	-268	0.99	AGCACCAATATATAGCAAGGCCGGCCATCAGAGTCATTTA**G**TCGAATGGA
-412	-362	0.98	TAAAAATATGTTAAAAAAGACCAAGGAAAAGGTACTGCTA**A**TCAATTGAA
-783	-733	1.00	AAAAGAAATATAAAAAAAGGGCATCATTTCCATCTCTTGT**G**AAATTTCTT
-1258	-1208	0.94	ATCTAAAGGATATAAACGCACCTGATCAAATTAGACAATA**T**CCAACGGTG
-1173	-1123	1.00	GAATTATCTATAAATAGAGACCCCCGAGACCCCCTACAAC**A**GTTCAAATC

Table 3
Predicted cis-acting elements of the *SinSyn* gene promoter (1520 bp)

Component Name	Sequence and Quantity	Position	Predictive Function
O2-site	GATGATG, 1	-1332	oxidative stress response element
TCT-motif	TCTTAC, 1	-245	part of a light responsive element
A-box	CCGTCC, 1	-1447	cis-acting regulatory elemente
Box 4	ATTAAT, 1	-1101	part of a conserved DNA module involved in light responsiveness
GC-motif	CCCCCG, 1	-1153	enhancer-like element involved in anoxic specific inducibility
CAAT-box	CAAT, 22	-16, etc.	common cis-acting element in promoter and enhancer regions
CCAAT-box	CAACGG, 1	-1216	MYBHv1 binding site
MSA-like	TCCAACGGT, 2	-1404, -1218	cis-acting element involved in cell cycle regulation
WUN-motif	AAATTTCTT, 1	-742	wound responsive element
MYB recognition site	CCGTTG, 1	-1504	drought response element
TC-rich repeats	ATTCTCTAAC, 1	-82	cis-acting element involved in defense and stress responsiveness
GATA-motif	AAGGATAAGG, 1	-390	part of a light responsive element
AuxRE	TGTCTCAATAAG, 1	-581	part of an auxin-responsive element
MYC	CAATTG, 1	-1435	adversity stress response elements
CGTCA-motif	CGTCA, 1	-1202	cis-acting regulatory element involved in the MeJA-responsiveness
AAAC-motif	CAATCAAAACCT, 1	-16	light responsive element
TATA-box	TATA, 14	-239, etc.	core promoter element around − 30 of transcription start

Analysis of promoter activity in transient transformed tobacco leave

The full-length promoter p0 and three 5' truncations (p1, p2, p3) promoter sequences were ligated upstream of the *GUS* gene through homologous recombination to produce recombinant plasmids Q0, Q1, Q2, and Q3. The recombinant plasmids were sent to the company for sequencing. The plasmids with correct sequencing results were retained and then transformed into *Agrobacterium tumefaciens*

GV3101. After GUS staining, stable blue spots were observed in the transiently transformed tobacco leaves (Fig. 4a), and all four promoter fragments exhibited promoter activity. Real-time fluorescence quantitative PCR was used to detect the relative expression of the *GUS* gene (Fig. 4b) and GUS enzyme activity (Fig. 4c). The positive control CaMV35s *GUS* gene exhibited the highest relative expression. Among the four promoter fragments, p1 had the highest activity, and the activity of p3 and p0 were lower than that of p2, which was consistent with the outcomes of GUS chemical tissue staining. It was assumed that − 956 bp ~ -622 bp was an important position of *pSinSyn*.

Screening and validation of transgenic Arabidopsis thaliana

Transgenic *Arabidopsis* seedlings of T1, T2, and T3 generations were screened on MS Hyg solid medium (Fig. 5a, b, c). Two-week-old seedlings were identified at the DNA molecular level. After PCR amplification, the expected fragment size was consistent with the target fragment (Fig. 5d, e). The results indicated that the positive transgenic *Arabidopsis thaliana* was successfully obtained.

GUS histochemical staining was conducted on transgenic plants containing various promoter fragments. As shown in Fig. 6 (6a, b, c, d, e), blue coloration was detected in the stems, leaves, pods, roots and flowers of transgenic *Arabidopsis*, indicating that the promoter did not exhibit obvious tissue specificity.

In order to quantitatively distinguish the expression of the *GUS* reporter gene in different transgenic lines, qRT-PCR analysis (Fig. 6f) and GUS enzyme activity analysis (Fig. 6g) were carried out. The *GUS* gene expression and GUS activity of the transgenic line CaMV35s were the strongest, and the activity of the four promoter fragments was p1 > p2 > p0 > p3. Compared with the results of tobacco transient expression, p0 and p3 exhibited the opposite phenomenon, which may be attributed to the differences in species.

Hormone-induced pSinSyn drives GUS gene expression

In further exploring the response of *pSinSyn* to hormone treatment, T3 homozygous transgenic *Arabidopsis* plants were treated with MeJA, NAA, and IBA. After treatment with 100 μM MeJA (Fig. 7a), compared with CK- and Q1, the Q0 responded rapidly to MeJA within 6 h, causing the expression of the *GUS* gene to reach its lowest value, and then continued to decrease. At 48 h, it slowly returned to normal levels. These results indicate that the promoter region between p0 and p1 (-1520 bp ~ -956 bp) contained a MeJA recognition element. Under NAA treatment (Fig. 7b), *GUS* gene expression in Q2 increased to the highest peak at 6 hours, and then returned to normal level at 12 h, indicating that the promoter contains the NAA-responsive element between p2 and p3 (-622 bp ~ -395 bp). Under the IBA treatment, the expression of *GUS* gene driven by p2 increased rapidly and reached the peak within 3 h, and then decreased at 6 h. However, it was still significantly up-regulated compared with that before the treatment (Fig. 7c). The response time was longer than that of NAA. Based on the above results, some elements of the promoter may respond to hormones. Once the element responds to hormones, it will affect the expression of the downstream *GUS* gene up or down in a certain period of time. When the stress effect is weakened, the gene expression will return to the baseline level.

GUS gene expression of various pSinSyn fragments under abiotic stress

Under 20% PEG treatment (Fig. 8a), there was no significant change in the expression level of *GUS* gene in Q0, Q1 and Q2 transgenic *Arabidopsis thaliana*. The expression level of GUS gene in Q3 transgenic *Arabidopsis* was significantly up-regulated at 6 h and 12 h, and peaked at 12 h. The results showed that the drought stress response element was located in the promoter − 395 bp ~ -1 bp interval. Under NaCl treatment (Fig. 8b), there was no significant difference in the expression of *GUS* gene in Q0 transgenic *Arabidopsis* under stress. The expression of *GUS* gene in Q1 transgenic *Arabidopsis thaliana* was significantly up-regulated at 24 h under stress, and remained at a high expression level at 48 h. The expression of GUS gene in Q2 transgenic *Arabidopsis* was significantly up-regulated, peaked at 12 h, and returned to the baseline level at 48 h. The expression of *GUS* gene in Q3 transgenic *Arabidopsis* was significantly up-regulated at 12 h and peaked at 24 h. According to the results, the position of the NaCl response element was located between − 956 bp and − 1 bp.

Discussion

The cis-acting elements in the promoter play a key role in regulating gene expression at the transcriptional level (Dao and Spicuglia. 2018; Hernandez-Garcia and Finer. 2014). A typical promoter contains not only the CAAT-box and TATA-box, which are essential for initiating gene transcription, but also other cis-acting elements that respond to various biotic and abiotic stresses, regulating the transcription of downstream genes (Cvetesic and Lenhard. 2017; Gill. 2001; Hong and Cohen. 2022). Some studies have investigated the function of response elements in the promoter by creating an expression vector with a promoter deletion fragment through recombination (Chang, et al. 2023; Lin, et al. 2022; Wang, et al. 2019; Zhou, et al. 2020).

SIN is a type of isoquinoline alkaloid (BIAs), and its structure is similar to morphine. SIN is primarily found in the rhizome of the plant, with a content of up to 2% (Yamasaki 1976). However, the long growth cycle of *Sinomenium acutum* is difficult for planting on a large scale. Based on the transcriptome and metabolome analysis of *Sinomenium acutum*, our research group speculated on the synthesis pathway of SIN in the early stages of our study. We identified and verified the related enzyme genes in the synthesis pathway, which further confirmed the biosynthesis pathway of SIN. Among them, SinSyn is the key enzyme in the biosynthesis pathway of SIN. Because sinoacutine is the starting site of the downstream synthesis pathway of SIN and the basic skeleton of SIN, the analysis of SinSyn synthetase is very important for the biosynthesis of SIN.

A 1520 bp promoter region was cloned to analyze the transcriptional regulation of the gene. A lot of cis-acting elements of typical promoters, such as TATA-box, CAAT-box, and other cis-acting elements of environmental and stress responses, were found in *pSinSyn*, according to bioinformatics study. Subsequently, three distinct 5' end deletion segments were cloned based on the distribution of cis-acting elements. The resulting promoters were then fused with the expression vector pCAMBIA1301 to create a fusion expression vector.

The obtained promoter activity was qualitatively analyzed using the transient expression analysis approach. The GUS tissue staining (Fig. 4a) demonstrated the activity of the obtained promoters. Concurrently, the findings of *GUS* gene expression (Fig. 4b) and GUS enzyme activity detection (Fig. 4c) confirmed that the *GUS* gene driven by the promoter deletion fragment p1 is the strongest at both transcriptional and translational levels, and the activity of p3 and p0 were lower than that of p2. It was assumed that the *pSinSyn* plays an important role in the region from − 956 bp to -622 bp.

The fusion expression vector was transformed into *Arabidopsis thaliana* by stable genetic transformation technology, and homozygous plants were screened. After 48 h, it began to slowly return to normal levels, indicating that the promoter responded to MeJA and was negatively regulated. It was also determined that the MeJA response element was located at -1520 bp ~ -956 bp. Under the treatment of auxin NAA and IBA, the expression of *the GUS* gene driven by the p2 promoter was significantly up-regulated in a certain period of time. The above results indicated that the promoter could be induced by auxin NAA and IBA, and the auxin response element was located at -622 bp ~ -395 bp.

Furthermore, under drought stress, the expression level of p3-driven *GUS* gene was up-regulated, which proved that the gene promoter could also respond to drought stress, and it was speculated that the response element was located between − 395 bp and − 1 bp of the promoter. Under salt stress, p1, p2 and p3 can drive *GUS* gene expression up-regulated, so the salt stress response element may be located between − 956 bp and − 1 bp.

In conclusion, our results confirmed that the *SinSyn* gene promoter could respond to methyl jasmonate (MeJA), auxin (NAA, IBA), drought treatments and salt treatments and the locations of responsive elements were provided.

Declarations

Ackonwledgements

This work was supported by Postgraduate Scientific Research Innovation Project of Hunan Province (QL20230167). Hunan Natural Science Foundation Project, No. 2020JJ4043 and No. 2022JJ50301. Industrial Innovation Chain Project, No. 2020SK1020. Huaihua City 's ' Unveil the list ' key research project, No. QY-0JZ1C03

Author contribution

AML, YH designed the study. AML and LB prepared material. AML conducted the experiments. AML, CJB and ZXY analyzed the data, AML and CXB prepared the manuscript. All authors read and approved the manuscript.

Data Availability

All data generated or analyzed during this study are included in this published article (and its additional files). Requests for material should be made to the corresponding authors

Conflict of Interest The authors declare that the research was conducted in the absence of any potential conflict of interest.

Informed consent Informed consent was not required as no human or animals was involved.

Research involving human and animal rights Our study has no research involved human participants or animals.

References

1. Ali I, Sher H, Ali A, Hussain S, Ullah Z (2022) Simplified floral dip transformation method of *Arabidopsis thaliana*. J Microbiol Methods 197:106492. https://doi.org/10.1016/j.mimet.2022.106492
2. Blázquez M (2007) Quantitative GUS Activity Assay of Plant Extracts. CSH Protoc. 2007:pdb.prot4690. https://doi.org/10.1101/pdb.prot4690
3. Chang X, Yang M, Li H, Wu J, Zhang J, Yin C, Ma W, Chen H, Zhou F, Lin Y (2023) Cloning of the promoter of rice brown planthopper feeding-inducible gene *OsTPS31* and identification of related cis-regulatory elements. Pest Manag Sci 79:1809–1819. https://doi.org/10.1002/ps.7356
4. Chen N, Xie R, Chen JP, Zhong YL, Zhang XW, Gui QW, Guo C, Yang H (2024) Proposal for the classification of sinomenine alkaloids. Fitoterapia 172:105713. https://doi.org/10.1016/j.fitote.2023.105713
5. Chen S, Qiu G (2020) Cloning and activity analysis of the promoter of nucleotide exchange factor gene *ZjFes1* from the seagrasses Zostera japonica. Sci Rep 10:17291. https://doi.org/10.1038/s41598-020-74381-6
6. Clough SJ, Bent AF (1998) Floral dip: a simplified method for *Agrobacterium*-mediated transformation of *Arabidopsis thaliana*. Plant J. https://doi.org/10.1046/j.1365-313x.1998.00343.x. 16:735 – 43
7. Cvetesic N, Lenhard B (2017) Core promoters across the genome. Nat Biotechnol 35:123–124. https://doi.org/10.1038/nbt.3788
8. Dao LTM, Spicuglia S (2018) Transcriptional regulation by promoters with enhancer function. Transcription. https://doi.org/10.1080/21541264.2018.1486150. 9:307 – 14
9. Dong G, Fan M, Wang H, Leng Y, Sun J, Huang J, Zhang H, Yan J (2023) Functional Characterization of *TkSRPP* Promoter in Response to Hormones and Wounding Stress in Transgenic Tobacco. Plants (Basel). 12: https://doi.org/10.3390/plants12020252
10. Gao WJ, Liu JX, Xie Y, Luo P, Liu ZQ, Liu L, Zhou H (2021) Suppression of macrophage migration by down-regulating Src/FAK/P130Cas activation contributed to the anti-inflammatory activity of sinomenine. Pharmacol Res 167:105513. https://doi.org/10.1016/j.phrs.2021.105513

11. Gill G (2001) Regulation of the initiation of eukaryotic transcription. Essays Biochem 37:33–43. https://doi.org/10.1042/bse0370033
12. Gong N, Wang L, An L, Xu Y (2023) Exploring the active ingredients and potential mechanisms of action of *Sinomenium acutum* in the treatment of rheumatoid arthritis based on systems biology and network pharmacology. Front Mol Biosci 10:1065171. https://doi.org/10.3389/fmolb.2023.1065171
13. He SM, Song WL, Cong K, Wang X, Dong Y, Cai J, Zhang JJ, Zhang GH, Yang JL, Yang SC, Fan W (2017) Identification of candidate genes involved in isoquinoline alkaloids biosynthesis in Dactylicapnos scandens by transcriptome analysis. Sci Rep 7:9119. https://doi.org/10.1038/s41598-017-08672-w
14. Hernandez-Garcia CM, Finer JJ (2014) Identification and validation of promoters and cis-acting regulatory elements. Plant Sci 217–218. https://doi.org/10.1016/j.plantsci.2013.12.007. :109 – 19
15. Hong CKY, Cohen BA (2022) Genomic environments scale the activities of diverse core promoters. Genome Res 32:85–96. https://doi.org/10.1101/gr.276025.121
16. Jefferson RA, Kavanagh TA, Bevan MW (1987) GUS fusions: beta-glucuronidase as a sensitive and versatile gene fusion marker in higher plants. Embo j 6:3901–3907. https://doi.org/10.1002/j.1460-2075.1987.tb02730.x
17. Kielkopf CL, Bauer W, Urbatsch IL (2020) Bradford Assay for Determining Protein Concentration. Cold Spring Harb Protoc. 2020:102269. https://doi.org/10.1101/pdb.prot102269
18. Kummari D, Palakolanu SR, Kishor PBK, Bhatnagar-Mathur P, Singam P, Vadez V, Sharma KK (2020) An update and perspectives on the use of promoters in plant genetic engineering. J Biosci 45:119. https://doi.org/10.1007/s12038-020-00087-6
19. Li C, Jiang W, Jiang X, Gai Y (2023) Cloning and functional analysis of the *PLkF3H2* promoter in *Larix kaempferi*. Plant Cell, Tissue and Organ Culture (PCTOC). 154:481 – 91. https://doi.org/10.1007/s11240-023-02467-w
20. Li RZ, Guan XX, Wang XR, Bao WQ, Lian LR, Choi SW, Zhang FY, Yan PY, Leung ELH, Pan HD, Liu L (2023) Sinomenine hydrochloride bidirectionally inhibits progression of tumor and autoimmune diseases by regulating AMPK pathway. Phytomedicine 114:154751. https://doi.org/10.1016/j.phymed.2023.154751
21. Lin M, Yan J, Ali MM, Wang S, Tian S, Chen F, Lin Z (2022) Isolation and Functional Characterization of a Green-Tissue Promoter in Japonica Rice (*Oryza sativa* subsp. *Japonica*). Biology (Basel). 11: https://doi.org/10.3390/biology11081092
22. Liu W, Zhang Y, Zhu W, Ma C, Ruan J, Long H, Wang Y (2018) Sinomenine Inhibits the Progression of Rheumatoid Arthritis by Regulating the Secretion of Inflammatory Cytokines and Monocyte/Macrophage Subsets. Front Immunol 9:2228. https://doi.org/10.3389/fimmu.2018.02228
23. Mavrodiev EV, Dervinis C, Whitten WM, Gitzendanner MA, Kirst M, Kim S, Kinser TJ, Soltis PS, Soltis DE (2021) A new, simple, highly scalable, and efficient protocol for genomic DNA extraction from diverse plant taxa. Appl Plant Sci 9:e11413. https://doi.org/10.1002/aps3.11413

24. Monika B, Parul G, Sanjay K, Singh AK (2016) The Promoter of AtUSP Is Co-regulated by Phytohormones and Abiotic Stresses in *Arabidopsis thaliana*. Front Plant Sci 7:1957. https://doi.org/10.3389/fpls.2016.01957
25. Rombauts S, Déhais P, Van Montagu M, Rouzé P (1999) PlantCARE, a plant cis-acting regulatory element database. Nucleic Acids Res 27:295–296. https://doi.org/10.1093/nar/27.1.295
26. Shirsat A, Wilford N, Croy R, Boulter D (1989) Sequences responsible for the tissue specific promoter activity of a pea legumin gene in tobacco. Mol Gen Genet 215:326–331. https://doi.org/10.1007/bf00339737
27. Wang C, Gao G, Cao S, Xie Q, Qi H (2019) Isolation and functional validation of the *CmLOX08* promoter associated with signalling molecule and abiotic stress responses in oriental melon, Cucumis melo var. makuwa Makino. BMC Plant Biol 19:75. https://doi.org/10.1186/s12870-019-1678-1
28. Wang S, Zhang L, Zhou Y, Liu Z, Zhou Z, Huang J (2023) A review on pharmacokinetics of sinomenine and its anti-inflammatory and immunomodulatory effects. Int Immunopharmacol 119:110227. https://doi.org/10.1016/j.intimp.2023.110227
29. Wang Y, Gao YH, Zhu YQ, Si JP (2019) Cloning and function analysis of promoter of *DcCDPK8* from *Dendrobium catenatum*. China J Chin Materia Med 44:293–297. https://doi.org/10.19540/j.cnki.cjcmm.20181106.005
30. Yamasaki H (1976) Pharmacology of sinomenine, an anti-rheumatic alkaloid from *Sinomenium acutum*. Acta Med Okayama 30:1–20
31. Zeng Xiyao Q, Kewei L, Yuyan Z, Xixin, Yang Hua and Xiong Xingyao (2019) Analyzed the synthesis pathway of sinomenine in *Sinomenium acutum* based on transcriptome sequencing. Chin Herb Med 50:8. https://doi.org/10.7501/j.issn.0253-2670.2019.22.023
32. Zhang C, Zhang S, Liao J, Gong Z, Chai X, Lyu H (2022) Towards Better Sinomenine-Type Drugs to Treat Rheumatoid Arthritis: Molecular Mechanisms and Structural Modification. Molecules 27. https://doi.org/10.3390/molecules27248645
33. Zhou L, Hao Y, Lu G, Wang P, Guo H, Cheng H (2020) Cloning and functional analysis of *AmDUF1517* promoter from *Ammopiptanthus mongolicus*. J Biosci Bioeng 130:233–238. https://doi.org/10.1016/j.jbiosc.2020.04.014
34. Zhu LP, Yu Z, Zou CX, Li QL (2010) Plant stress-inducible promoters and their function. Yi Chuan. https://doi.org/10.3724/sp.j.1005.2010.00229. 32:229 – 34

Figures

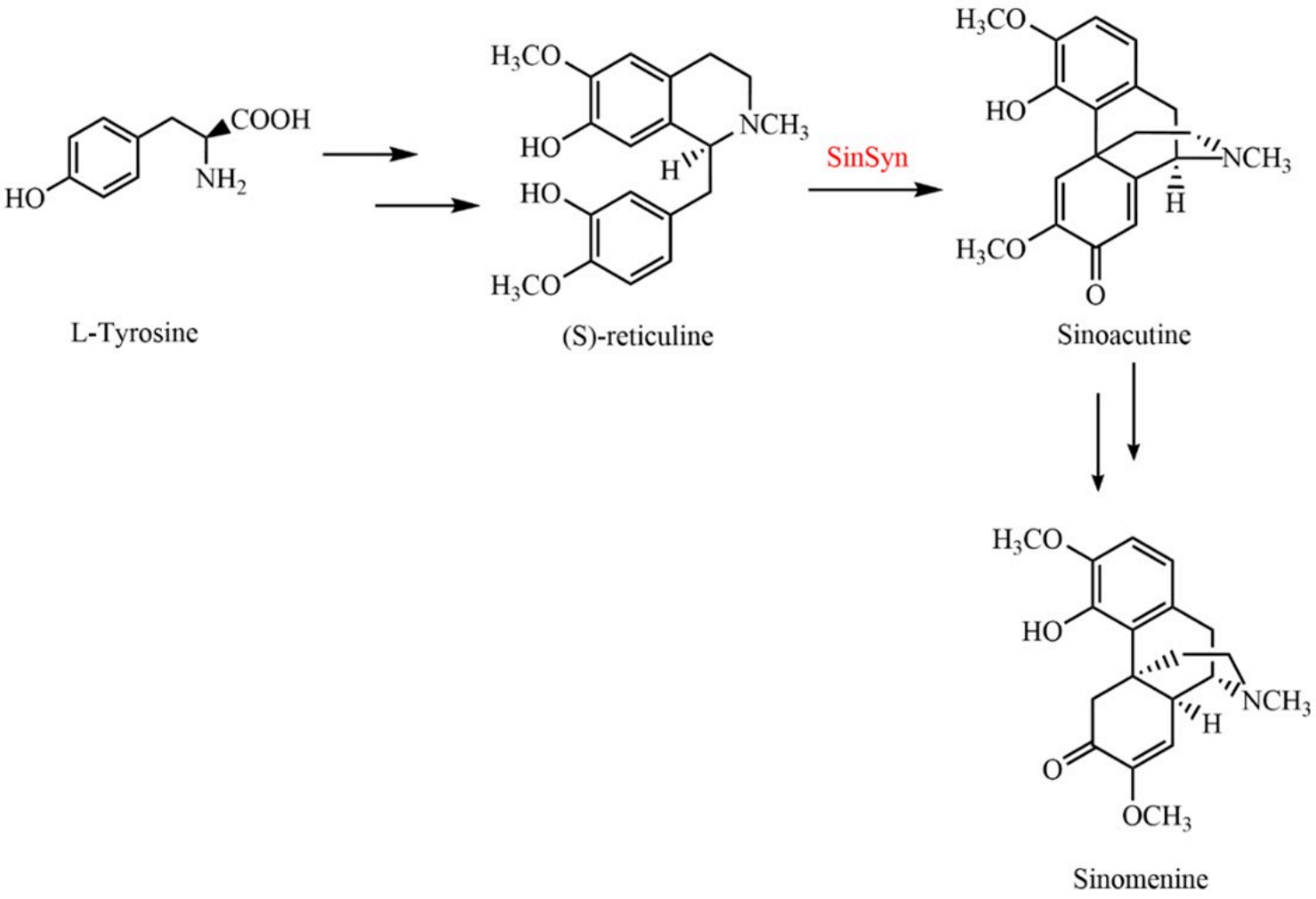

Figure 1

Schematic diagram of Sinoacutine synthetase (SinSyn) catalyzing (S)-reticuline annonine to Sinoacutine

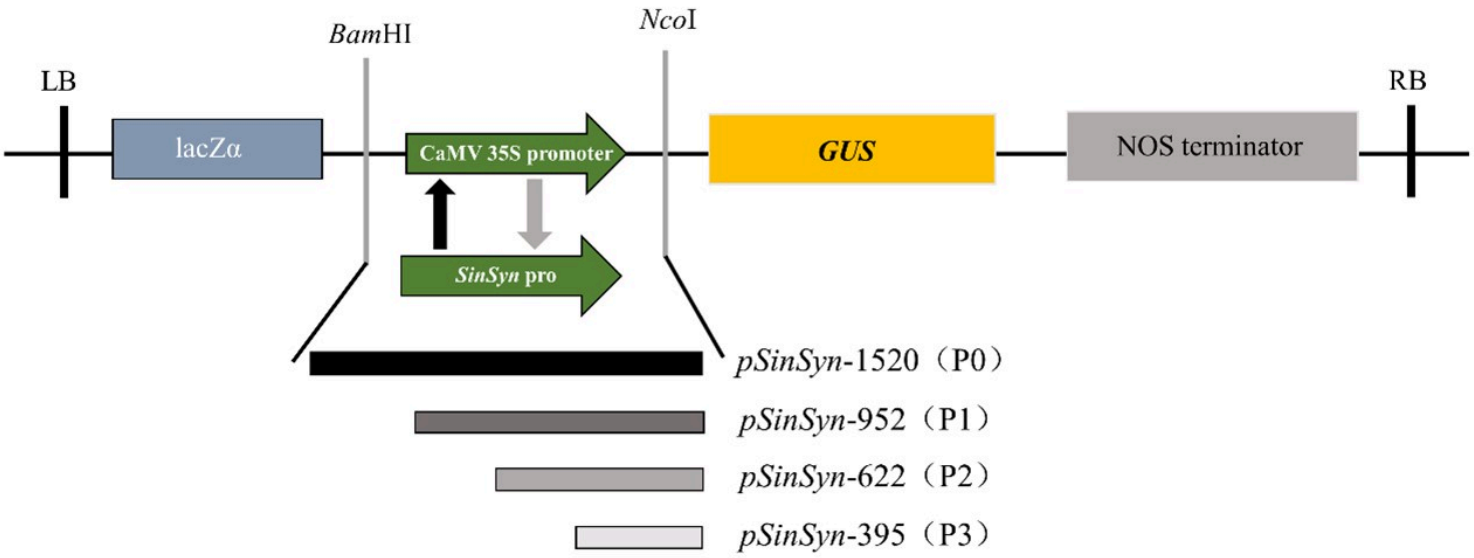

Figure 2

Schematic diagram showing the full length promote of *pSinSyn* and its deletion vectors construction.

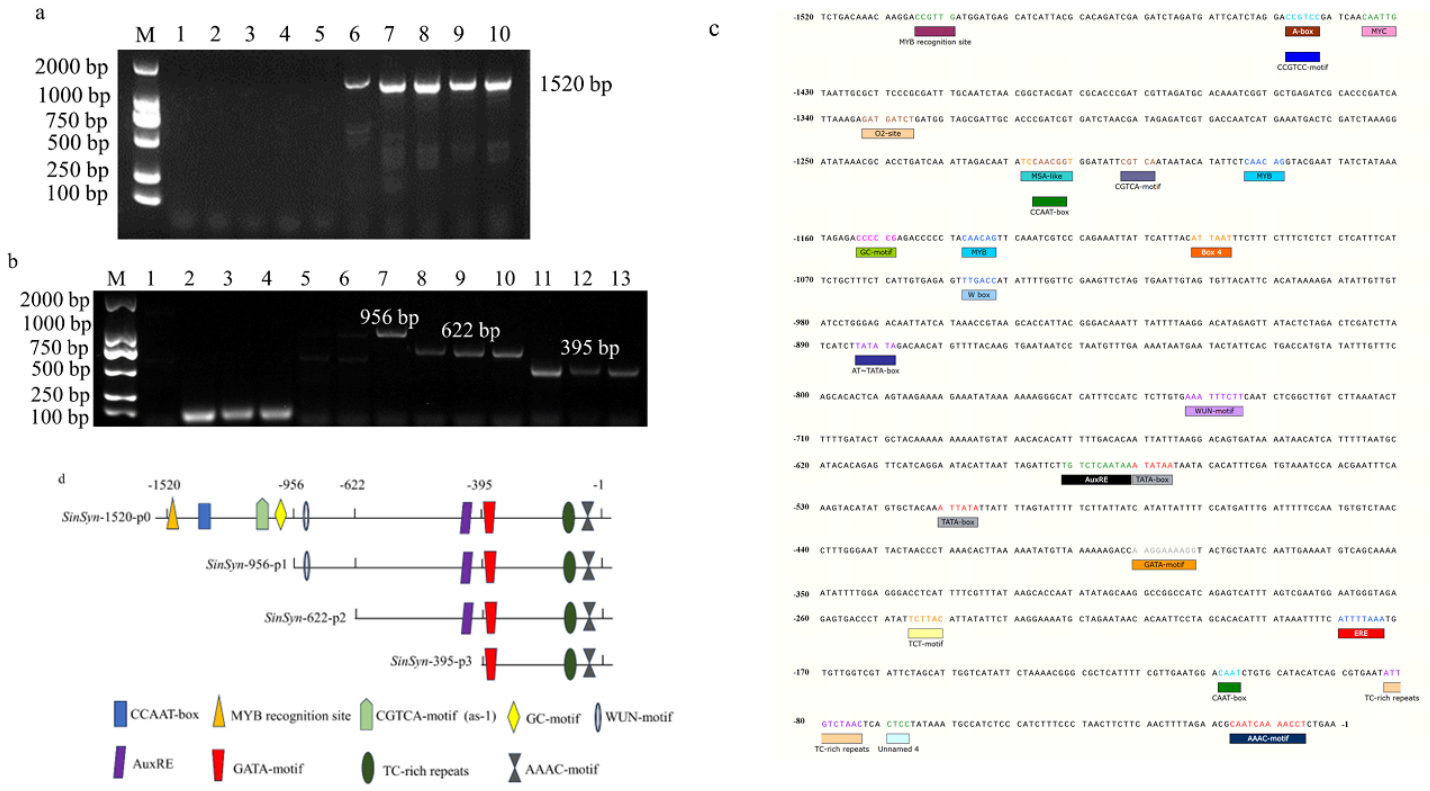

Figure 3

(a) Promoter p0 amplification. M: Marker DL2000, lane 1-5: the first round of nested PCR, lane 6-10: the second round of nested PCR. (b) Amplification of promoter fragments p1, p2, p3. M: Marker DL2000, lane 2-4: positive control, lane 5-7: p0, lane 8-10: p2, lane 11-13: p3. (c) The 5' upstream promoter sequences of the *SinSyn* gene. Numbers indicate the positions relative to the start codon ATG. (d) Schematic diagram of *SinSyn* promoter structure of four different lengths

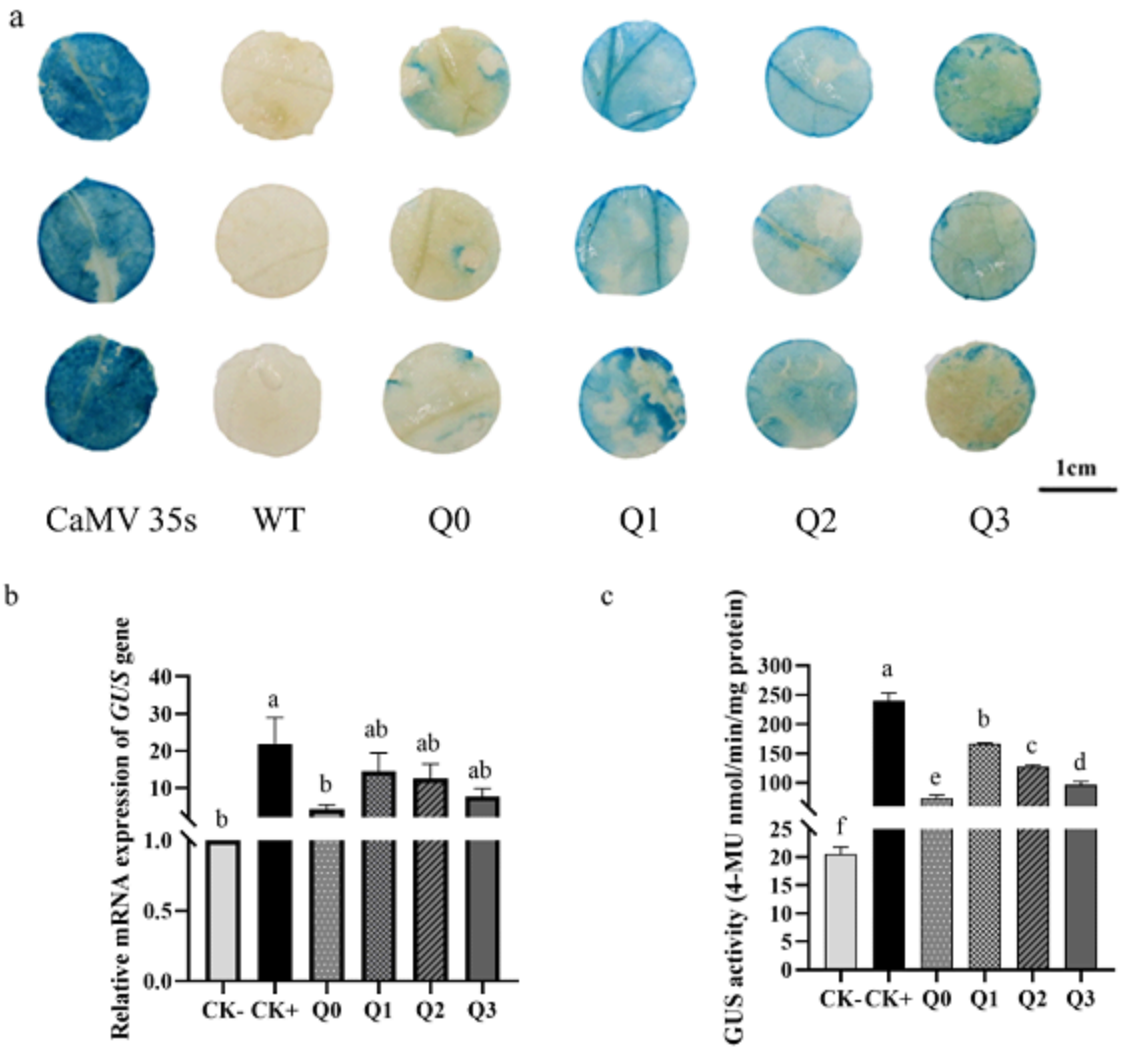

Figure 4

Promoter activity verification. (a) *SinSyn* promoter series transiently transforms tobacco GUS staining. (b) Analysis of relative expression of *GUS* gene in transiently transformed tobacco with *SinSyn* promoter series. (c) Analysis of the GUS enzyme activity of *SinSyn* promoter series transiently transformed tobacco

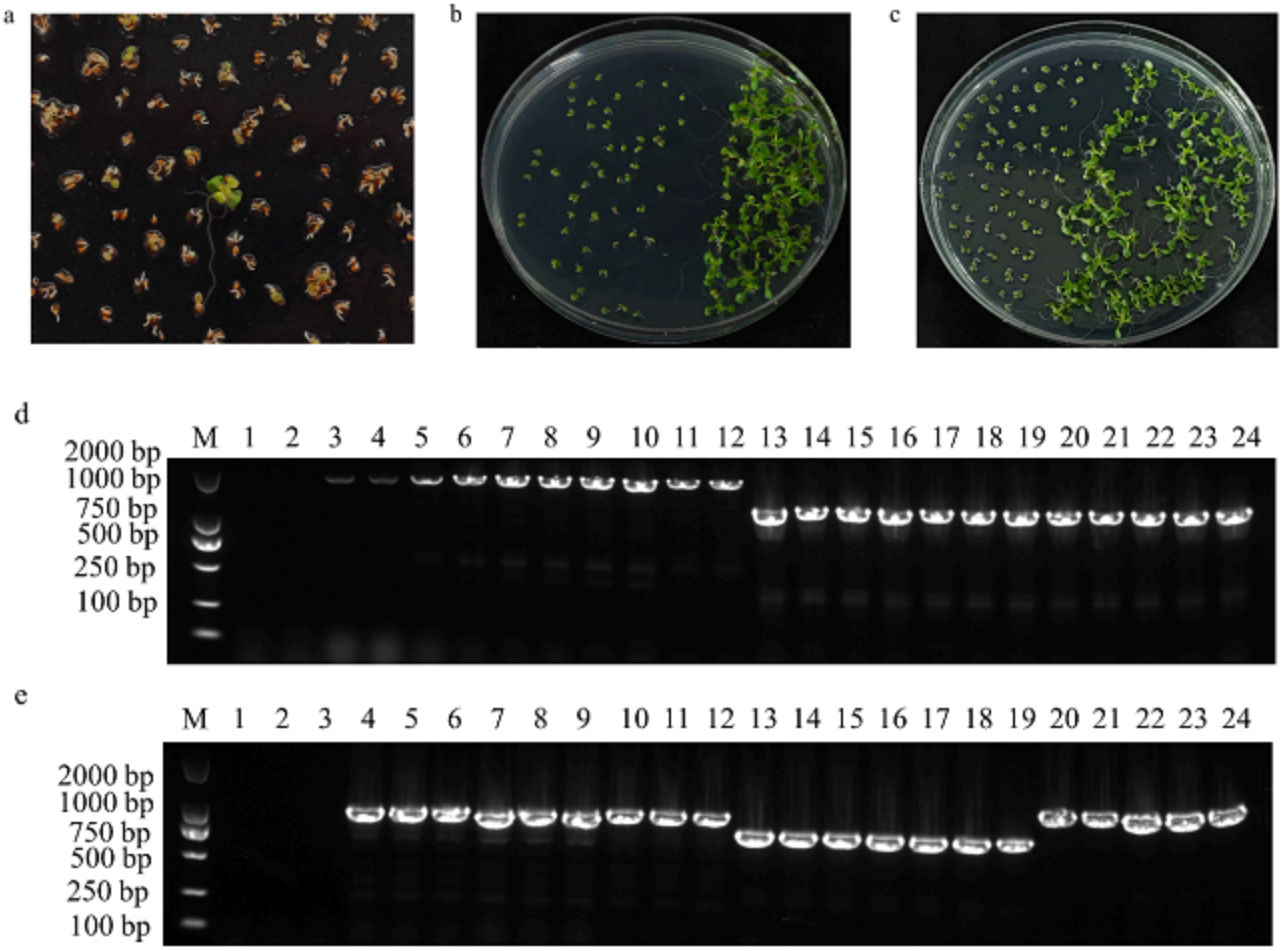

Figure 5

Screening and verification of transgenic *Arabidopsis thaliana* (a) T1. (b) T2 (col-0 on the left). (c) T3 (col-0 on the left). (d) lane 1-2 negative control (col-0). lane 3-12 Q0 (1880 bp); lane 13-24 Q1 (1324 bp). (e) lane 1-3 negative control (col-0); lane 4-12 Q2 (990 bp); lane 13-19 Q3 (773 bp); lane 20-24 positive control (1163 bp).

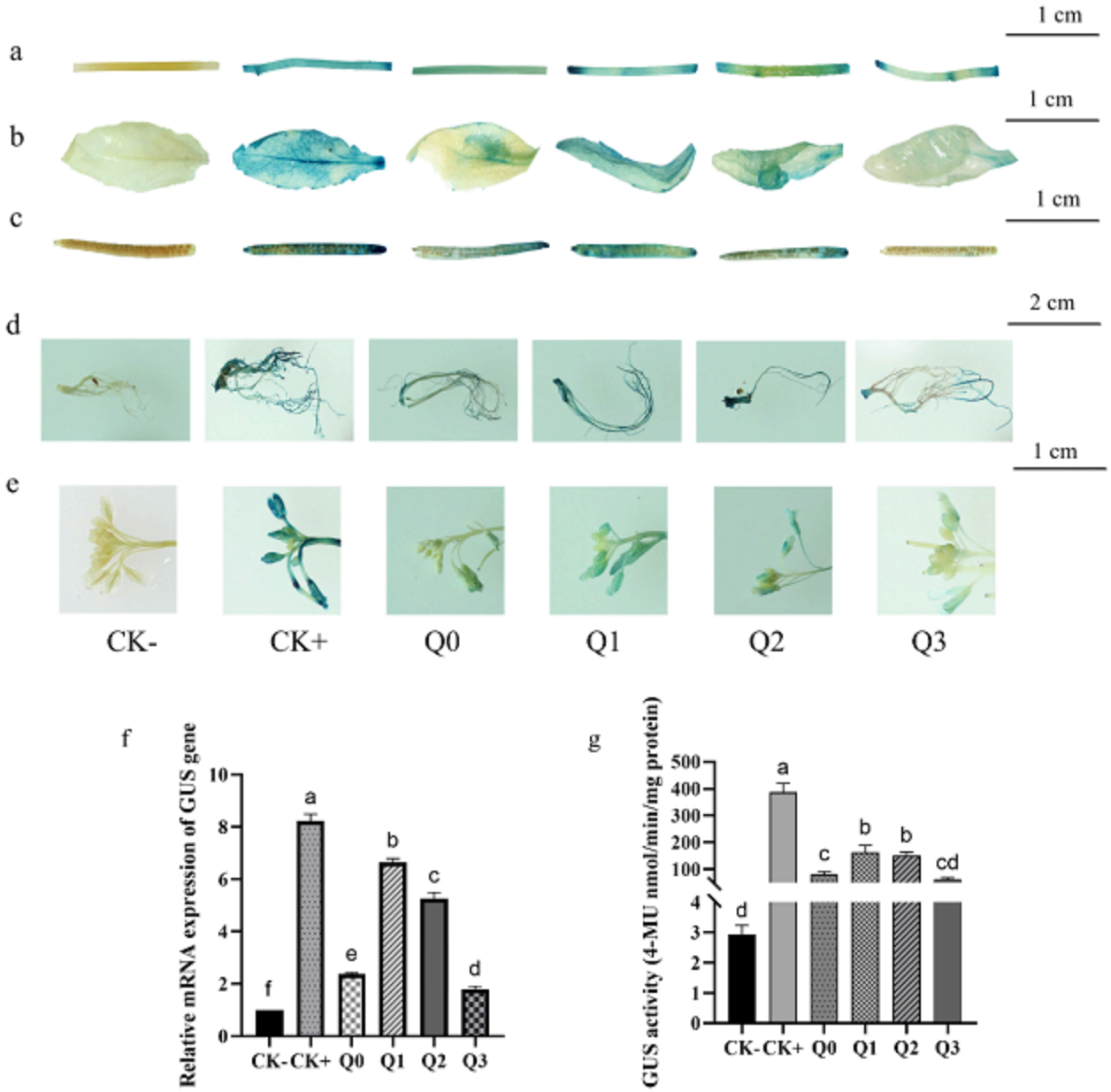

Figure 6

GUS staining analysis of transgenic *Arabidopsis*. (a)stems. (b) leaves. (c) fruit pods. (d) roots. (e) flowers under normal conditions. From left to right in turn is CK-: wild-type *Arabidopsis*. CK+: positive control pCAMBIA 1301 empty vector. Q0-Q3: transgenic *Arabidopsis* with corresponding promoter fragment fusion vectors

(f) Analysis of *GUS* gene expression driven by promoters of different lengths under normal conditions. (g) Detection of GUS activity of different promoter fragments under normal conditions

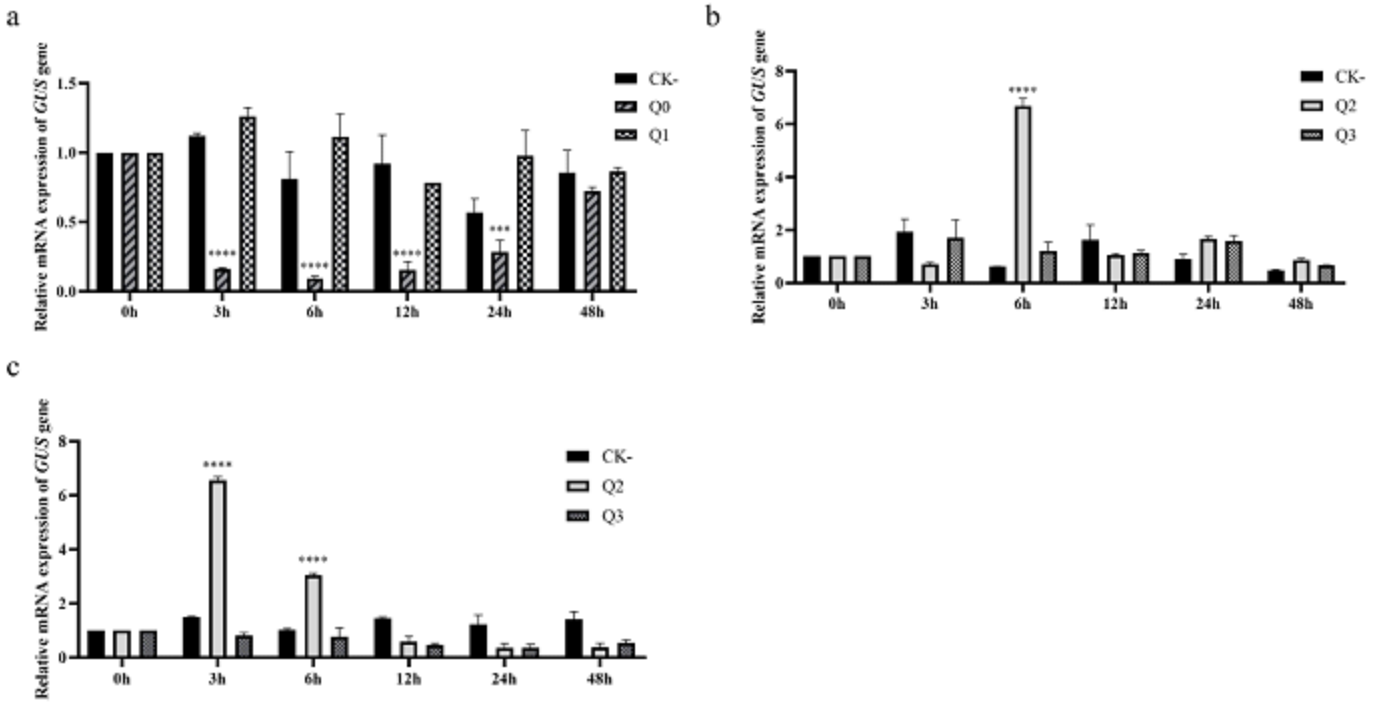

Figure 7

The relative expression level of *GUS* gene after hormones treatment of transgenic *Arabidopsis thaliana*. (a)100 μM MeJA. (b) 100 μM NAA. (c) 100μM IBA

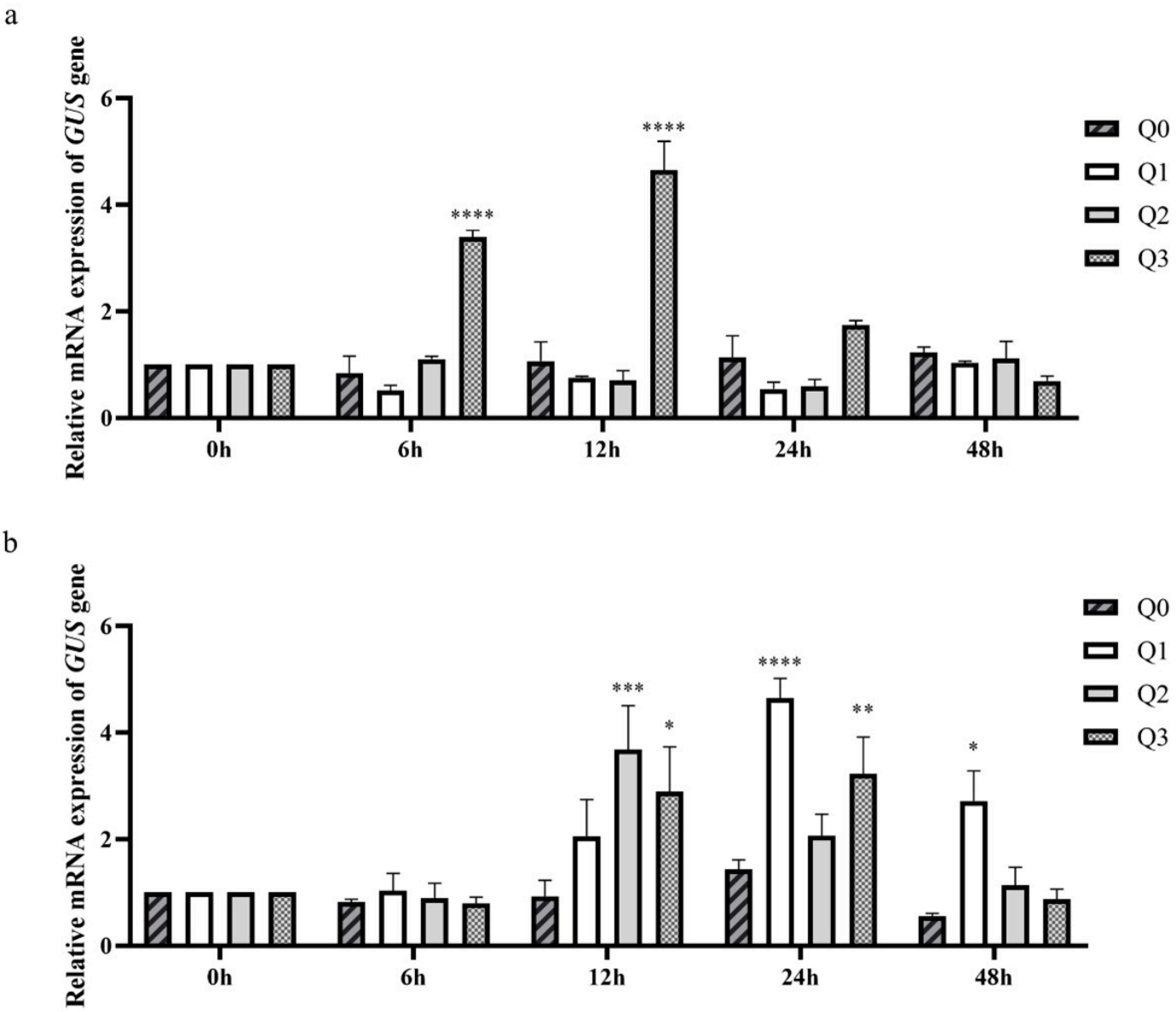

Figure 8

Relative expression levels of *GUS* genes in transgenic *Arabidopsis* after treatment with (a) 20% PEG and (b)10 g/L NaCl, respectively